


 CrossMark
click for updates

 Cite this: *Soft Matter*, 2015,
11, 7441

DOI: 10.1039/c5sm90153g

www.rsc.org/softmatter

Correction: Wrapping of ellipsoidal nano-particles by fluid membranes

Sabyasachi Dasgupta, Thorsten Auth and Gerhard Gompper

 Correction for 'Wrapping of ellipsoidal nano-particles by fluid membranes' by Sabyasachi Dasgupta *et al.*, *Soft Matter*, 2013, **9**, 5473–5482.

Phase transitions have been calculated for ellipsoidal particles with various aspect ratios. The values for the adhesion strength for the transitions depend on both particle size and aspect ratio. Calculations are conveniently carried out for fixed small axes of prolate particles or long axes of oblate particles, fixed surface area, or fixed volume. We have calculated adhesion strengths for transitions between partially-wrapped and completely-wrapped states using particles with the same surface area A , and adhesion strengths for binding of the particles to the membrane using particles with the same length of their small axis a . The data is plotted as a function of the reduced adhesion strength $\tilde{w} = 2wa^2/\kappa$. In the original publication, we missed a factor $4\pi a^2/A$ in the scaling of the values for the effective adhesion strength for calculations with fixed surface area. In addition there is a misprint in eqn (5), the corrected equation is:

$$\frac{\Delta E(A_{\text{ad}}/A, \tilde{w})}{\pi\kappa} = f\left(\frac{A_{\text{ad}}}{A}\right) - \frac{\tilde{w}A}{2\pi a^2} \frac{A_{\text{ad}}}{A}. \quad (5)$$

In Fig. 4, 7, 8 and 11 of the original publication, the numerical values for the adhesion strengths of all phase boundaries except W_1 have to be multiplied by $4\pi a^2/A$. Corrected labels are S_{21} (0.53), E(4.76), W_2 (5.23) and S_{22} (9.31) in Fig. 4(a) and S_{21} (1.28), E(6.78), W_2 (7.73) and S_{22} (12.49) in Fig. 4(b). Corrected Fig. 7, 8 and 11 are provided, where $\tilde{w} = 2wa^2/\kappa$ and $\tilde{\sigma} = \sigma a^2/\kappa$. The transitions shift to smaller adhesion strengths for prolate particles, where a is the short axis, and to larger adhesion strengths for oblate particles, where a is the long axis. For spherical particles $4\pi a^2/A = 1$, therefore the results presented in Fig. 3 remain unaffected.

The phase diagrams presented here are most easily interpreted for ellipsoidal particles with fixed length of the axis a , because of the choice of \tilde{w} for the reduced adhesion strength. Instead, in the original Fig. 11, the W_2 transition is shown for reduced adhesion strength $\tilde{w} = wA/(2\pi\kappa)$, which can be most easily interpreted for particles with fixed surface area A . Almost all data presented in the corrected figures can be rescaled to be used for particles with fixed A – besides the transition for $\tilde{\sigma} = 2$ in Fig. 11 that applies only for fixed length of the small axis. In the corrected Fig. 11, the transition W_2 for prolate ellipsoids is almost independent of the particle aspect ratio; the increased bending energy cost to wrap the tips of the ellipsoidal particles with higher aspect ratio is compensated for by the increased adhesion energy gain because of the larger particle surface area.

The Royal Society of Chemistry apologises for these errors and any consequent inconvenience to authors and readers.



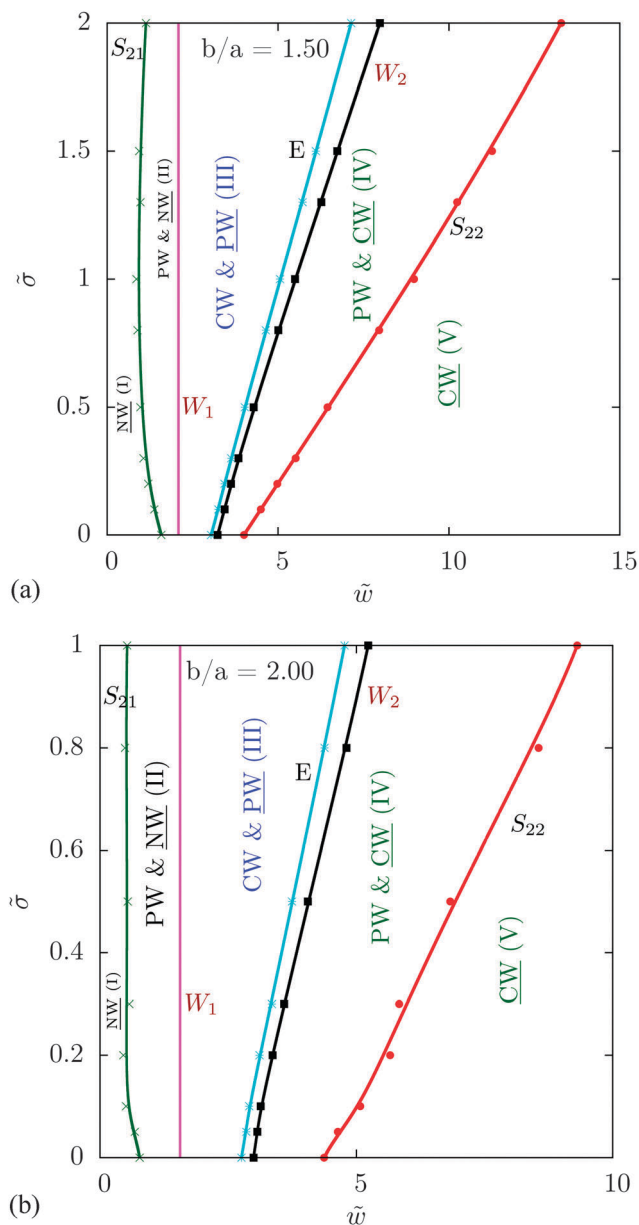


Fig. 7 Wrapping states for prolate ellipsoidal particles with aspect ratios (a) 1.5 and (b) 2, plotted analogously to Fig. 6.



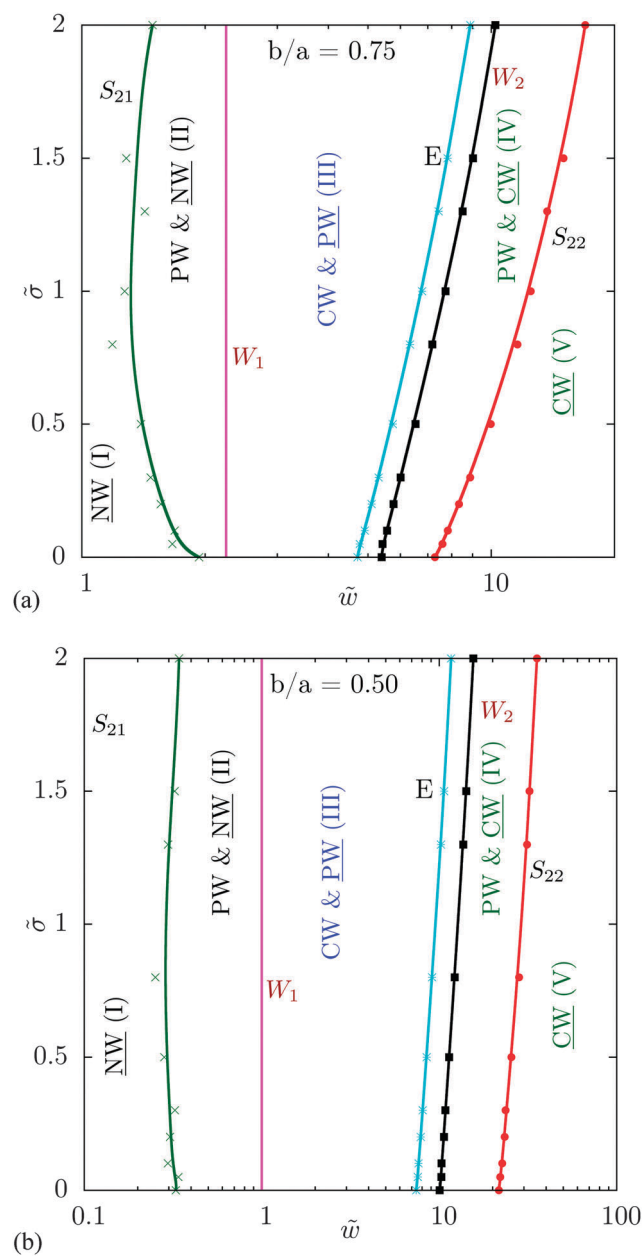


Fig. 8 Wrapping states for oblate ellipsoidal particles with aspect ratios (a) 0.75 and (b) 0.5, plotted analogously to Fig. 6.



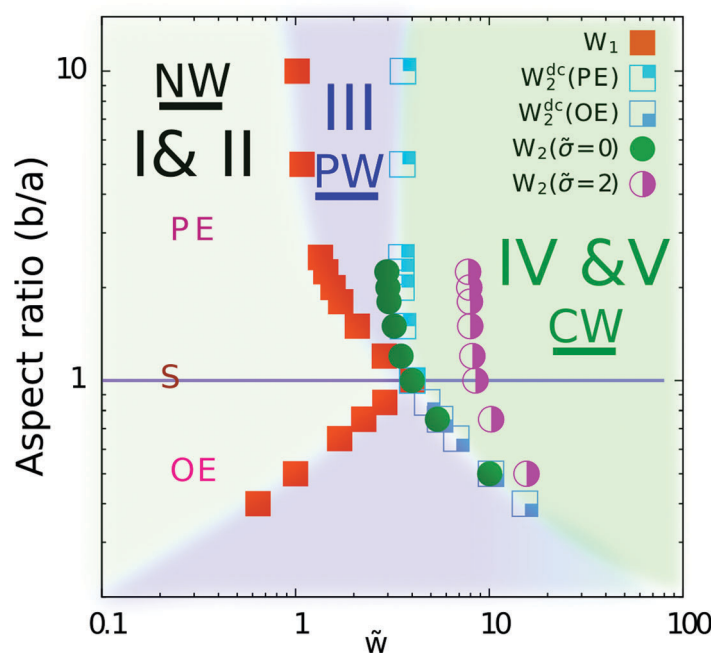


Fig. 11 Stable wrapping states for different aspect ratios b/a , reduced adhesion strengths \tilde{w} , and for $\bar{\sigma} = 0$ and for $\bar{\sigma} = 2$. Prolate ellipsoids (PE) have aspect ratios $b/a > 1$, while oblate ellipsoids (OE) have aspect ratios $b/a < 1$. Stable wrapping states are the non-wrapped state (NW), the partially-wrapped state (PW), and the completely-wrapped state (CW); the roman numbers correspond to those used in Fig. 6–8. For blue open squares labeled with index dc, the deformed catenoid approximation has been used.

